Hybrid-effect transmission enhancement induced by oblique illumination in nano-ridge waveguide

Jen-Yu Fang[1], Chung-Hao Tien[2], and Han-Ping D. Shieh[2]

[1]*Department of Photonics and Institute of Electro-Optical Engineering*
[2]*Department of Photonics and Display Institute*
National Chiao Tung University, Hsinchu 30010, Taiwan
ryfang.eo91g@nctu.edu.tw

Abstract: In a nano-ridge waveguide under oblique illumination, we demonstrated transmission enhancement resulting from a hybrid effect between propagation modes and surface plasmon wave. The measured near-field intensity with 44-degree illumination was 1.6 times higher than that illuminated with normal incident light. Consequently, a wedge-shaped fiber probe was proposed to serve as a compact near-field light source.

OCIS codes: (050.1220) Apertures; (240.6680) Surface plasmons; (120.7000) Transmission; (210.0210) Optical data storage.

References and links

1. T. W. Ebbesen, H. J. Lezec, H. F. Ghaemi, T. Thio, and P. A. Wolff, "Extraordinary optical transmission through sub-wavelength hole arrays," Nature **391**, 667-669 (1998).
2. H. J. Lezec, A. Degiron, E. Devaux, R. A. Linke, L. Martin-Moreno, F. J. Garcia-Vidal, and T. W. Ebbesen, "Beaming light from a subwavelength aperture," Science **297**, 820-822 (2002).
3. E. Popov, M. Neviere, J. Wenger, P.-F. Lenne, H. Rigneault, P. Chaumet, N. Bonod, J. Dintinger, and T. Ebbesen, "Field enhancement in single subwavelength apertures," J. Opt. Soc. Am. A **23**, 2342-2348 (2006).
4. Y. Xie, A. R. Zakharian, J. V. Moloney, and M. Mansuripur, "Transmission of light through periodic arrays of sub-wavelength slits in metallic hosts," Opt. Express **14**, 6400-6413 (2006).
5. X. Shi, R. L. Thornton, and L. Hesselink, "Ultrahigh light transmission through a C-shaped nanoaperture," Opt. Lett. **28**, 1320-1322 (2003).
6. X. Shi and L. Hesselink, "Design of a C aperture to achieve l/10 resolution and resonant transmission," J. Opt. Soc. Am. B **21**, 1305-1317 (2004).
7. A. V. Itagi, W. A. Challener, I. K. Sendur, and T. E. Schlesinger, "Finite difference frequency domain scattered field formulation for near field optical data storage," in *Proc. of SPIE* **5380**, 351-359 (2004).
8. K. Sendur, C. Peng, and W. Challener, "Near-field radiation from a ridge waveguide transducer in the vicinity of a solid immersion lens," Phys. Rev. Lett. 94, 043901(4) (2005).
9. K. Sendur and P. Jones, "Effect of fly height and refractive index on the transmission efficiency of near-field optical transducers," Appl. Phys. Lett. **88**, 091110(4) (2005).
10. L. Sun and L. Hesselink, "Low-loss subwavelength metal C-aperture waveguide," Opt. Lett. **31**, 3606-3608 (2006).
11. Y. Xie, A. R. Zakharian, J. V. Moloney, and M. Mansuripur, "Optical transmission at oblique incidence through a periodic array of sub-wavelength slits in a metallic host," Opt. Express **14**, 10220-10227 (2006).
12. A. R. Zakharian, J. V. Moloney, and M. Mansuripur, "Surface plasmon polaritons on metallic surfaces," Opt. Express **15**, 183-197 (2006).
13. P.-K Wei, Y.-C. Huang, C.-C. Chieng, F.-G. Tseng, and W. Fann, "Off-angle illumination induced surface plasmon coupling in subwavelength metallic slits," Opt. Express **13**, 10784-10794 (2005)
14. Y.-C. Chen, J.-Y. Fang, C.-H. Tien, and H.-P. D. Shieh, "Extraordinary optical transmission enhancement of asymmetric nanoaperture with surface corrugation," in *Proc. Int. Symp. Optical Memory 2005*, (Honolulu, 2005).
15. Y.-C. Chen, J.-Y. Fang, C.-H. Tien, and H.-P. D. Shieh," High-transmission hybrid-effect-assisted nanoaperture," Opt. Lett. **31**, 655-657 (2006).
16. Y.-C. Chen, J.-Y. Fang, C.-H. Tien, and H.-P. D. Shieh, "Double-Corrugated C-Shaped Aperture for Near-Field Recording," Jpn. J. Appl. Phys. **45**, 1348-1350 (2006).
17. H. Raether: Surface Plasmons on Smooth and Rough Surfaces and on Gratings (Springer, New York, 1988).

#83523 - $15.00 USD Received 30 May 2007; revised 24 Jul 2007; accepted 24 Jul 2007; published 30 Aug 2007

1. Introduction

Achieving sub-wavelength optical resolution beyond the diffraction limit is of critical importance to many fields, such as optical storage and nanolithography. A practical solution is to confine light with a sub-wavelength aperture on metal film. Unfortunately, for a sub-wavelength aperture, low power transmission always accompanies the shrinkage of the aperture size which corresponds to spot size. To dissolve this theoretic constraint, some research addressed the transmission enhancement through sub-wavelength apertures as a result of surface plasmon resonance [1-4]. An aperture array or a single hole surrounded by a periodic structure was fabricated on metal film to induce surface plasmon resonance in the dielectric-metal interface. Meanwhile, studies on transmission through a specifically-designed nano-waveguide have also been reported [5-10]. Owing to the boundary conditions, incident light was coupled into propagation modes instead of evanescent waves and suffered from less energy dissipation along waveguides. Recently, more attentions have been paid to the mutual interaction between surface plasmon resonance and propagation modes [11-13]. We presented a hybrid effect in which surface plasmon waves and propagation modes coexist in a ridge waveguide surrounded by a corrugated structure [14-16]. To characterize the photon capturing capability of the waveguide, the transmission was represented by power throughput (PT). The power throughput is defined as the ratio of the transmitted power through a waveguide to the incident power on the aperture area in the absence of the waveguide. As a result, the power throughput of this novel design was able to be further enhanced over four orders of magnitude higher than a conventional aperture. However, the proposed design was difficult to fabricate. Therefore, in this paper, we present a simpler approach to enhance the transmission by illuminating a ridge waveguide on metal film with obliquely incident light. Both far-field and near-field measurement results proved the transmission enhancement under obliquely incident illumination. A wedge-shaped fiber probe demonstrated the hybrid effect and can be used as a novel near-field light source.

2. Modeling

In a smooth air-metal interface, surface plasmon waves cannot be excited by incident light because of the mismatch between the momentum of incident light and that of the surface plasmon wave. Either the attenuated total reflection (ATR) or a periodic structure in the dielectric-metal interface can induce the excitation [17]. By combining a ridge waveguide with a corrugated structure, we demonstrated a hybrid effect where both surface plasmon waves and propagation modes constructively contributed to the power throughput enhancement through the waveguide [15]. The hybrid effect implies that the surface plasmon wave would be able to contribute to an increase in the transmission of a ridge waveguide when the attenuated total reflection occurs in the dielectric-metal interface. The transmission of a ridge waveguide with obliquely incident illumination is schematically illustrated in Fig. 1(a). A 200-nm silver film on a glass substrate was perforated with a C-aperture and illuminated by a transverse-magnetic (TM) plane wave, which can be presented by *Ez*, *Ey* and *Hy*, respectively. The complex refractive index of the silver film was assumed to be 0.135 + 3.988i and that of the glass substrate was 1.475 at a free-space wavelength of 633nm. The dimensions of the waveguide are shown in Fig. 1(b). The Finite-Difference Time Domain method (FDTD) was employed to calculate the power throughput at a spacing of 50 nm from the exit plane of the waveguide and simulate the field distribution.

Our calculation showed that as the incident angle Φ impinging on the waveguide changed from 0 to 45 degree, the power throughput increased significantly and reached a peak of 3.5 at 44 degree, which is 2.3 times higher than that with normally incident light, as shown in Fig. 2. In the case of refractive index of the dielectric substrate of 1.475, the critical angle of the total internal reflection in the air-dielectric interface is 42.7 degree. When the dielectric substrate was covered with a metal film, the reflection coefficient of a TM wave dropped suddenly to a

#83523 - $15.00 USD Received 30 May 2007; revised 24 Jul 2007; accepted 24 Jul 2007; published 30 Aug 2007

minimum as the incident light impinged on the metal film at 44.5 degree, slightly above the critical angle. The dip in the reflectivity exhibited the excitation of surface plasmons in the interface. The coincidence between the incident angles of the minimum reflection coefficient and maximum power throughput indicated enhancement resulted from the surface plasmons excitation.

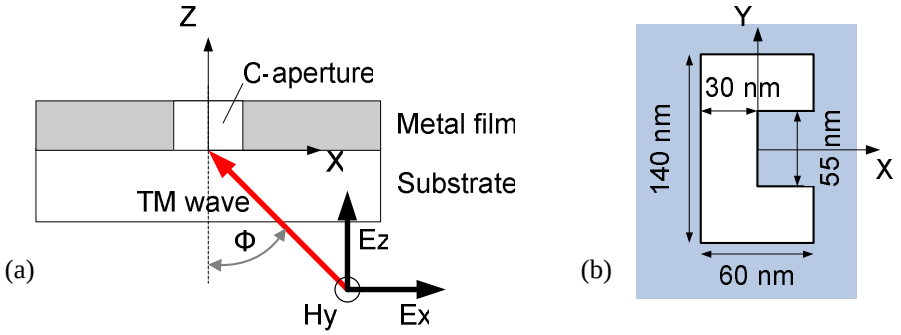

Fig. 1. (a) Schematic illustration of the optical model and (b) the dimensions of the C-aperture

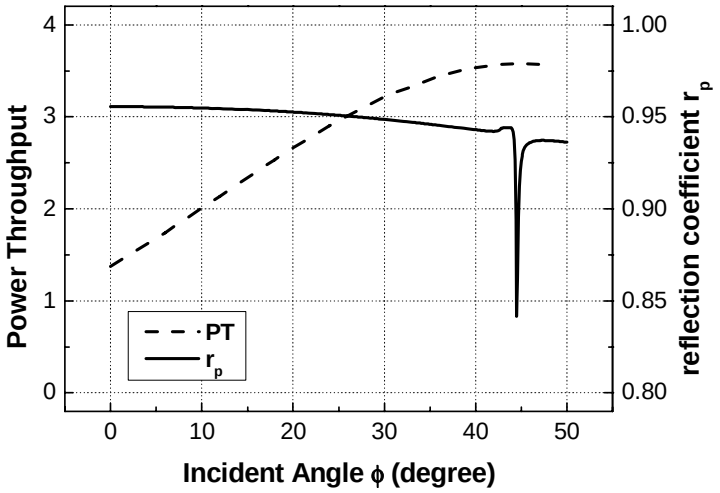

Fig. 2. The power throughput (PT) at a distance of 50 nm from the aperture and reflection coefficient r_p as a function of the incident angle

The calculated *Ex*, *Ez*, *Hy* field profile and magnitude of Poynting vector |*S*| distribution with 44-degree incident illumination are shown in Figs. 3(a) to (d). The results further revealed the existence of the hybrid effect between the propagation modes along the waveguide and the surface plasmons waves on the metal surface. From Fig. 3(a), the *Ex* field profile showed light propagating through the gap of the ridge waveguide along the z direction. The *Ez* field perpendicular to the metal surface yielded the surface plasmons wave along the surface on both sides, as shown in Fig. 3(b). We found that the waveguide functioned as a channel so that surface plasmons wave could be excited at the exit of the waveguide. The corresponding wave vector k_x which lies parallel to the surface could be described as

#83523 - $15.00 USD Received 30 May 2007; revised 24 Jul 2007; accepted 24 Jul 2007; published 30 Aug 2007

$$k_x = k_0 \left(\frac{\varepsilon_m \cdot \varepsilon_d}{\varepsilon_m + \varepsilon_d}\right)^{1/2} \tag{1}$$

where ε_m is dielectric constant of the metal film, ε_d is that of the dielectric material and k_0 is the wave vector of incident light. Then the surface plasmon wavelength λ_{SP} along the x direction can be obtained by

$$\lambda_{SP} = \frac{2\pi}{k_x} \tag{2}$$

According to Eq.(2), the corresponding surface plasmon wavelength in the dielectric-metal interface, $\lambda_{sp\ d\text{-}m}$, is 0.39 μm and that in the air-metal interface, $\lambda_{sp\ a\text{-}m}$, is 0.61 μm, which are in agreement with the FDTD simulation results, as shown in Fig. 3(b).

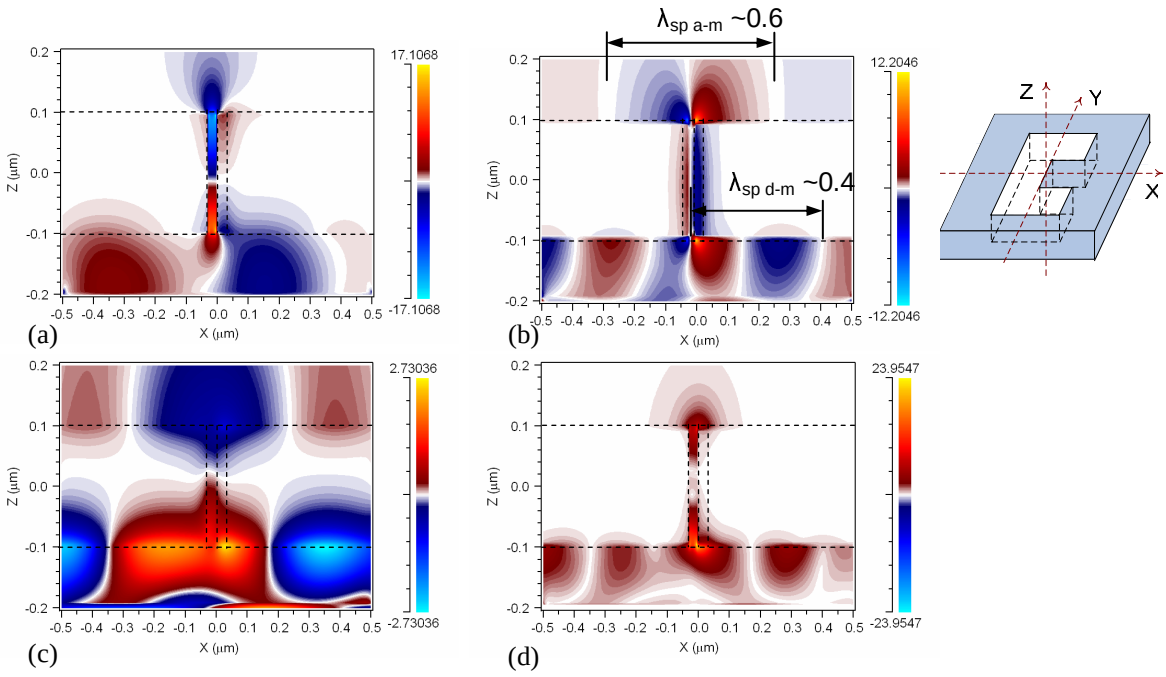

Fig. 3. (a) Ez, (b) Ex, and (c) Hy field profile, and (d) magnitude of Poynting vector plot when the incident angle is 44 degree. The dashed line showed the contours of the metal film and the C-aperture.

The magnitude of Poynting vector $|S|$ shown in Fig. 3(d) represented the energy flow in both $\pm x$ direction and $+z$ direction. The calculation showed that the incident energy was coupled into surface plasmon waves along the surface of entrance plane, captured by the waveguide and then propagated through the waveguide. The surface plasmon wave contributed to the increase of energy capturing ability and the propagation modes reduced the energy loss when light propagated through the waveguide. The hybrid effect between surface plasmon waves and propagation modes significantly enhance the transmission through the nano-aperture.

To further study the coupling between the incident light and the surface plasmon waves, the spectral response of the power throughput with 44-degree illumination in visible light region was also calculated, as presented in Fig. 4. The peak at the incident wavelength of 633 nm in the spectrum exhibits the surface plasmons excitation at a specific resonant wavelength.

#83523 - $15.00 USD Received 30 May 2007; revised 24 Jul 2007; accepted 24 Jul 2007; published 30 Aug 2007

The maximum power throughput indicates the energy transfer from the incident light to the surface plasmon waves. Then the surface plasmon wave constructively coupled with the propagation modes of the waveguide. The interaction between surface plasmon waves and propagation modes further increased the power delivered through the waveguide.

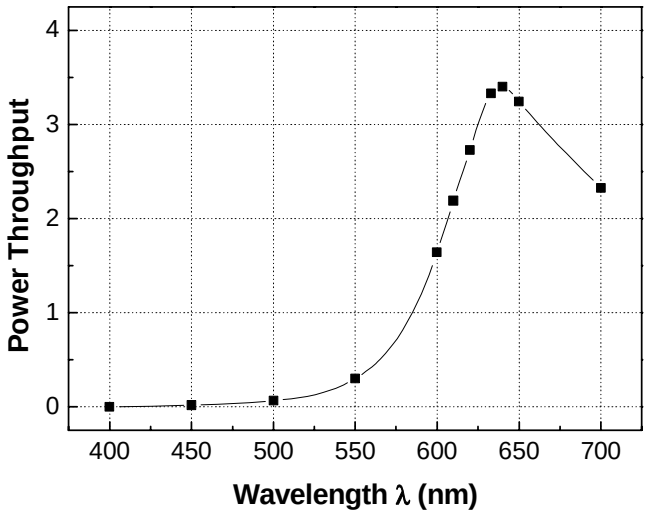

Fig. 4. The spectral response of the power throughput through the ridge waveguide with incident angle of 44 degree

The calculated electric intensity distribution inside the waveguide confirmed the existence of the propagation mode along the waveguide. Figs. 5(a), (b), and (c) represent the electric intensity distribution at a position of 1/4, 1/2, and 3/4 of the waveguide length from the entrance side. The mode field distribution remained when the light propagated along the waveguide. Moreover, the electric field was confined to the gap area and also penetrated into the ridge. Therefore, the gap and the ridge dimensions determined the supported propagation mode and the transmission through the waveguide. The propagation mode also contributed to the transmitted power propagation out of the waveguide. The calculation of the power throughput as a function of the distance from the waveguide in Fig. 5(d) showed the power throughput can keep over 1 within a spacing of 300 nm, which is larger than a conventional aperture, which is usually lower than 10^{-3} for a 60-nm square aperture.

The power throughput of a ridge waveguide under oblique illumination is only half of that surrounded by a corrugated structure with normally incident illumination. The mechanism was investigated by observing the power throughput illuminated with 44-degree incident light but with waveguide dimensions shrunk or enlarged. We defined the scale factor as the ratio of the modified dimension of the C-aperture to the original one, which is shown in Fig. 1(b). Then the power throughput as a function of the scale factor was obtained, as plotted in Fig. 6. The simulation results clearly showed the power throughput reached a peak of 4.8 as the dimensions shrank by a factor of 0.83 but dropped to 1.8 as the dimensions scaled up by 1.25. Compared to the original design which was optimized for normal incident illumination, the dimensionally scaling-down design further increased the power throughput by a factor of 1.42. According to waveguide theory, the dimensions of the ridge waveguide determine the propagation modes through the waveguide. In addition, the incident angle also dominates the coupling efficiency between the incident light and the propagation modes in the ridge waveguide. Consequently, in the original design, the enhancement from the surface plasmon

#83523 - $15.00 USD Received 30 May 2007; revised 24 Jul 2007; accepted 24 Jul 2007; published 30 Aug 2007

waves was offset by a reduction in the coupling efficiency due to oblique illumination. In contrast, dimensionally scaling-down altered the supported modes within the waveguide and thus the power throughput increased until the incident wavelength fulfilled the cut-off condition.

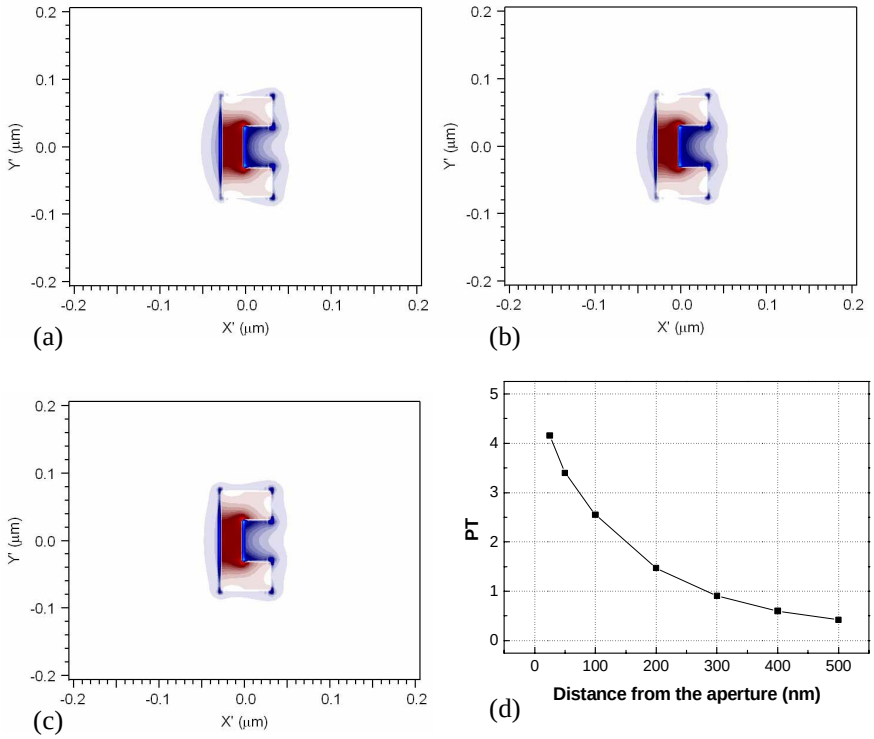

Fig. 5. The electric intensity distribution inside the waveguide at a position of (a) 1/4, (b) 1/2, (c) 3/4 of the length from the entrance plane when the light propagated along the waveguide, and (d) the power throughput decay as a function of the distance from the waveguide

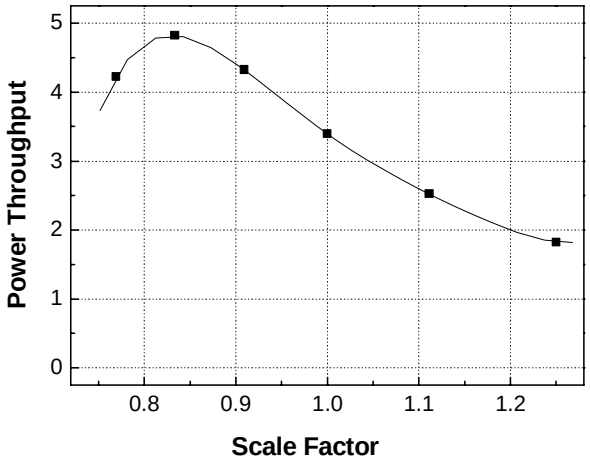

Fig. 6. Power throughput as the waveguide scales up or down by the scale factor in the model of 44-degree illumination

#83523 - $15.00 USD Received 30 May 2007; revised 24 Jul 2007; accepted 24 Jul 2007; published 30 Aug 2007

3. Experimental Results

To demonstrate the enhancement caused by the hybrid effect, we measured far-field power throughput and near-field optical intensity distribution of a ridge waveguide with normally and 44-degree incident illumination. In our experiment, a silver film with a thickness of 200 nm was coated with a glass substrate with a refractive index of 1.475 and perforated with a C-aperture, as shown in Fig. 7, by focused ion beam milling. A linearly polarized laser beam was focused on the aperture with a specific incident angle. The incident wave had a Gaussian distribution. However, the focused beam was assumed to have a planar wave front with equal amplitude on the effective area around the aperture because the focused spot was much larger than the dimensions of the aperture. In addition, the ratio of the measured transmitted power to the total incident power represented the overall power transmission. To coincide with the power throughput used in the simulation, the central peak value of the Gaussian beam was assumed to be the field amplitude at the aperture. The transmitted power was measured and then the calculated power throughput was compared to the simulation results accordingly. Furthermore, the near-field distribution measurement was performed by a near-field scanning optical microscope (NSOM), of which the spatial resolution was around 50 nm.

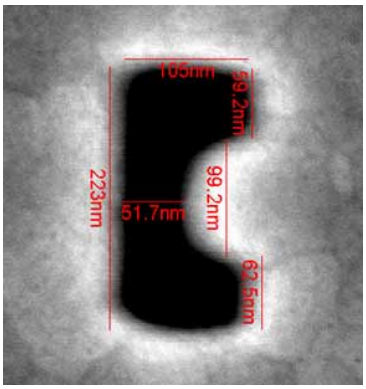

Fig. 7. SEM photo of the ridge waveguide

The measured far-field power throughput illuminated with normal incident light was 0.25 while that with 44-degree incident illumination was 0.33, which yielded an enhancement factor of 1.3. The hybrid effect reduced the energy decay from the exit of the waveguide and thus made the far-field power throughput detectable. The near-field distribution measurement also confirmed the enhancement. Figs. 8(a) and (b) showed the near-field distribution with normally and 44-degree incident illumination. From the measurement results, the spot sizes were estimated around 0.2~0.3 μm. Due to finite spatial resolution of NSOM of around 50 nm in this case, the measured spot size was larger than the simulated one, which was 0.2 μm. Moreover, since the measurement was made under the same setting-up condition, the signal amplitude represented the relative optical intensity emitted from the waveguide. By comparing the signal voltage of 1.1V in the normal-incidence model to that of 1.8V model under 40-degree incidence, the near-field enhancement factor can be as high as 1.6.

To examine the consistency of the experimental results with simulation, the power throughput and intensity distribution at 50 nm from the nano-waveguide with the dimensions of Fig. 7 were calculated with normally and 44-degree incident illumination. The simulation results are shown in Fig. 9. The output spot of the aperture with 44-degree incident illumination had a smaller size with higher peak intensity than that illuminated with normally incident light. The calculated power throughput enhancement as a result of the hybrid effect was 2.2. Moreover, the calculated *Ex* and *Ez* field profile under 44-degree illumination also

#83523 - $15.00 USD Received 30 May 2007; revised 24 Jul 2007; accepted 24 Jul 2007; published 30 Aug 2007

showed the hybrid effect in Fig. 10, even though the dimensions of the fabricated waveguide were larger than the optimal design. The incident light propagated through the waveguide with the aid of the surface plasmon waves in the dielectric-metal interface. Therefore, although the measured enhancement was not as high as the simulated one of 2.3, the results demonstrated that the surface plasmon waves induced by oblique illumination contributed to the enhancement of the transmitted power propagated through the ridge waveguide.

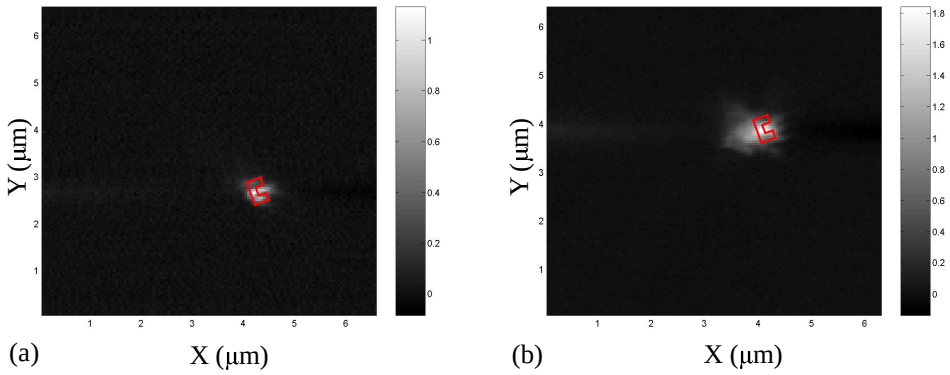

Fig. 8. Near-field distribution observed by NSOM with (a) normally and (b) 44-degree incident illumination while the red line represented the contours of the C-aperture

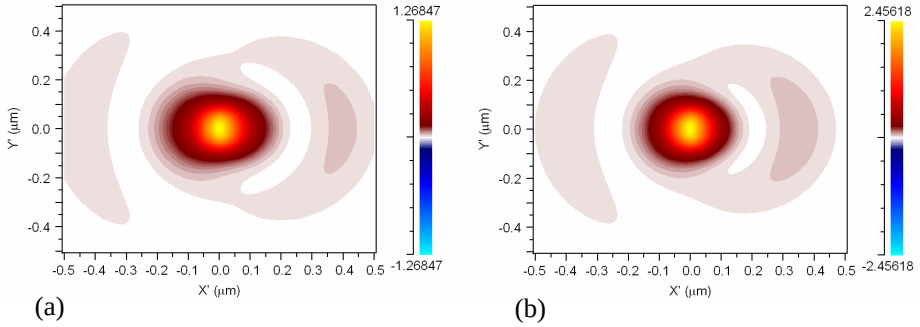

Fig. 9. Calculated electric intensity distribution at 50nm from the nano-waveguide with the fabricated dimensions with (a) normally and (b) 44-degree incident illumination

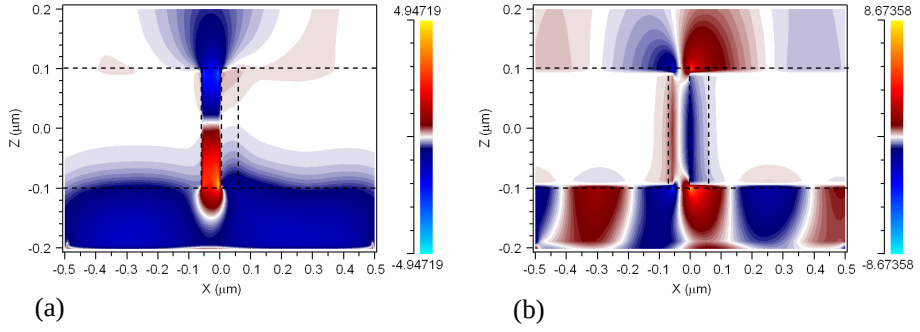

Fig. 10. Calculated (a) Ex and (b) Ez field profile with the fabricated dimensions

#83523 - $15.00 USD Received 30 May 2007; revised 24 Jul 2007; accepted 24 Jul 2007; published 30 Aug 2007

According to the hybrid effect demonstrated, a wedge-shaped fiber probe with a 45-degree wedge angle was fabricated, as shown in Fig. 11 (a). The wedge was made by diamond sawing at a controlled angle and covered with a sputtered silver film. The far-field transmission measurement setup is illustrated in Fig. 11 (b). A 1x2 coupler provided a reference port which was used to calculate the incident power on the aperture in the presence of a metal film covering the end face of the fiber probe port. The measured transmission efficiency, defined as the ratio of far-field output power through an aperture on a silver film on the end face of fiber probe to the incident power on the aperture, can reach 0.017. For conventional fiber probes, the transmission usually ranges from 10^{-3} to 10^{-5}. Our wedge-shaped fiber probe can enhance the transmission at least ten times higher than that of conventional probes and be used as a compact near-field light source for many applications.

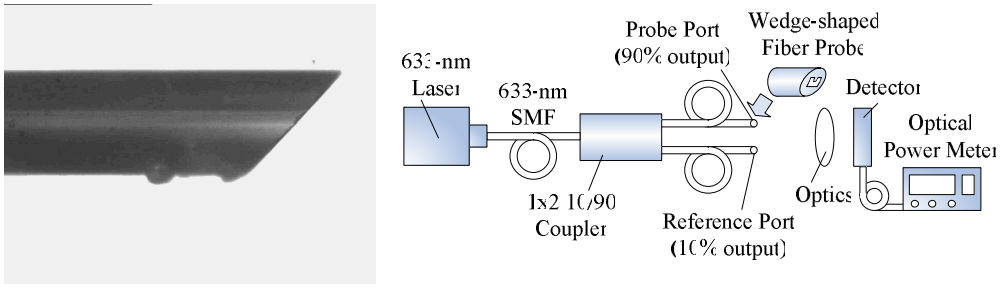

(a) (b)

Fig. 11. (a) Microscopic photo of a wedge-shaped fiber probe with a 45-degree wedge angle and (b) configuration of measurement setup

4. Conclusions

The transmission enhancement from the hybrid effect between the propagation modes and the surface plasmon waves was demonstrated and further confirmed by introducing attenuated total reflection with oblique illumination in a metal-dielectric interface. An enhancement factor of 1.6 in the near-field model and that of 1.3 in the far-field case with oblique illumination started an alternative approach to overcome the theoretic barrier that limits power transmission. Our proposed novel wedge-shaped fiber probe opens a new avenue to high-transmission near-field light sources.

Acknowledgments

The authors thank Dr. Pei-Kuen Wei of the Research Center of Applied Science, Academia Sinica, for assistance with the NSOM measurement. This research is partially supported by the National Science Council, Taiwan, for Promoting Academic Excellence of the University in "Photonics Science and Technology for Tera Era," under grant NSC 97-2752-E-009-009-PAE.

#83523 - $15.00 USD Received 30 May 2007; revised 24 Jul 2007; accepted 24 Jul 2007; published 30 Aug 2007